

# Numerical Simulation Research on Coupling Mechanism of Shield-Support-Surrounding Rock in Complex Loess Geology

Guoping LIU<sup>b</sup>, Jun FENG<sup>a</sup> and Heyi LIU<sup>a1</sup>

<sup>a</sup>China Institute of Water Resources and Hydropower Research, Beijing 100048, China

<sup>b</sup>Hanjiang-to-weihe river valley water diversion project construction CO.LTD.,  
Xian 710024, China

**Abstract.** The tunneling machine for the Hanjiang to Weihe River Water Diversion Project is expected to encounter complex and unpredictable geological conditions, which could result in accidents such as large deformations of soft rock and segment failure. To address this, a refined numerical simulation model using FLAC3D was utilized to study the coupling mechanism of shield-support-surrounding rock under loess geological conditions. Results show that the overall rock deformation is significant, but due to the support effect of the face, displacement at the cutter head is minimal. Deformation of the surrounding rock increases gradually from the back of the face to the pipe segment. Stress redistribution occurs within a certain range of the gap reserved at the shield, with the maximum principal stress in the secondary stress located near the tail of the shield. A typical cave section of Bailu Tableland exhibits a layered stress distribution phenomenon, with stress release from the cave wall to the outer rock mass. This includes zones of concentration, transition zones, and non-interference zones. In the excavation direction of the tunnel, the maximum principal stress is relatively high at the junction of the shield tail and the segment structure, as well as at the entrance of the tunnel.

**Keywords.** Hanjiang to Weihe River Water Diversion Project; Loess stratum; Shield structure; FLAC3D

## 1. Introduction

When tunnel excavation is carried out in loess strata [1], as the surrounding rock of most tunnel sections is saturated loess, if mining method is used, deformation and damage phenomena such as collapse of top arch, sliding of side wall, flowing mud at the foot of wall and bulging of bottom slab may occur [2][3], while shield method can achieve better safety and economic benefits [4][5].

Shield method is a mechanized construction method [6] in which shield machinery is pushed underground, supported by shield shells and pipe sheets to prevent the surrounding rock from collapsing into the tunnel, while excavating the soil with cutting devices in front of the excavation, and assembling prefabricated concrete pipe sheets to

---

<sup>1</sup> Corresponding author: Heyi LIU, China Institute of Water Resources and Hydropower Research, Beijing 100048, China; E-mail: heyiliu0914@163.com

form the tunnel structure, which has the advantages of less impact on the surrounding environment [7], less surface settlement caused by excavation [8], faster digging speed, better tunnel forming quality [9], high mechanization, reliable support lining quality [10][11] during construction and less affected by weather. From the end of the 19th century to the middle of the 20th century, shield machine technology achieved rapid development. At present, Japan is the most advanced country in the world in shield tunneling technology. The Technical Committee of Japanese Shield Construction Method has acknowledged 11 shield construction technologies, namely: mud and water pressurized shield construction method, bubble shield construction method, ECL (extruded concrete lining) construction method, MF shield construction method, DOT construction method, expanded shield machine construction method, Hollen construction method, Coulomb construction method, H&V shield construction method, MSD construction method, free section shield construction method, and eccentric multi-axis shield construction method.

In the Hanjiang to Weihe River Water Diversion Project, the strata traversed by the shield tunnel include quaternary loess, strongly weathered mudstone, loessial loam and multilayered paleosoil, sandstone, mudstone, conglomerate, biotite plagioclase gneiss, biotite granite, etc. The strata are complex and changeable, which are highly likely to cause large deformation of soft rock, shield tunneling machine stuck, and segment damage. At the same time, it is also the difficulty and hot spot in the research of engineering and academia [12]. Based on the background of tunnel engineering in the loess tableland, this paper studies the coupling mechanism of shield, support and surrounding rock under complex loess geological conditions by using FLAC3D refined numerical simulation model, so as to provide theoretical and technical support for the safe and smooth progress of the project.

## 2. Engineering Background

The south and north trunk lines of the Hanjiang to Weihe River Water Diversion Project pass through Shaoling Tableland, Bailu Tableland, Shenhe Tableland and Weibei Loess Tableland, with long crossing distance and complex geological conditions. The tunnel in the loess Tableland is a circular section, with the excavation diameter of 5.1m, segment thickness of 35cm and inner diameter of 4.4m. The types of surrounding rocks in each tunnel section are shown in Table 1 below:

**Table 1.** Statistical table of tunnel surrounding rock categories

Tunnel name	Surrounding rock categories	Lithology	Length (m)	Percentage of total length
Shenhe Tableland	V	Quaternary loess	2855	100%
Shaoling Tableland	V	Quaternary loess	8660	100%
Bailu Tableland	V	Quaternary loess, Neogene sandstone, mudstone	6930	71.2%
	IV	Neogene mudstone	2440	28.8%

### 3. Refined Simulation Model Relying on FLAC3D

Shenhe Tableland Cave segment, Shaoling Tableland Cave segment and Bailu Tableland Cave segment of the southern trunk line are the research objects. Since the whole engineering area is too large, typical cave segment with local maximum buried depth is selected for simulation in the study, and local geological structure is ignored. During the calculation, the surrounding rocks of Shenhe Tableland and Shaoling Tableland are generalized into Class V, part of the surrounding rocks of Bailu Tableland are generalized into class V and part of the surrounding rocks are generalized into class IV, and the numerical calculation model is established according to the tunnel size and the equipment parameters of the machine designed in the project.

#### 3.1. Parameter Selection

The geometric dimensions and technical parameters of the shield tunneling machine in actual engineering are shown in Table 2 below:

**Table 2.** Geometric dimensions and related technical parameters of shield tunneling machine

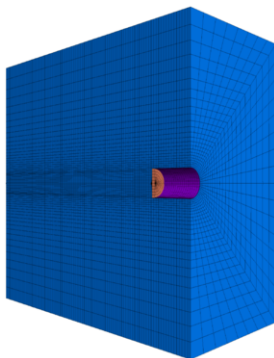
Diameter of excavation / cutter head (m)	Outer diameter of shield (m)	Segment outside diameter/cavity diameter (m)	Cutter head/shield length (m)	Shield thickness (m)	Segment width/thickness (m)	Cutter head maximum thrust (kN)
5.37	5.34	5.1/4.4	0.7/8.97	0.06	1.5/0.35	3476

The material of cutter head, front shield and backing is steel, and the material of segment is reinforced concrete. In the process of tunneling by shield machine, the pores between the lining segment of the body tail and excavated rock mass are grouting backfilled. During modeling, all the built-in structures of cutter head and shield section are converted to the equivalent weight of cutter head and shield. The weight of the supporting facilities after the shield tunneling machine and the related slag discharging and conveying system and other structures are converted to the weight of the precast segment. The technical parameters of the main components of the shield tunneling machine (equivalent weight in brackets) and the material parameters of the segment structure and grouting backfilling are shown in Table 3 below:

**Table 3.** Material parameters of main components

Component	Elastic modulus (GPa)	Poisson's ratio	Density (g/cm <sup>3</sup> )
Cutter head (steel)	206	0.3	7.8(5.3)
Front and rear shields (steel)	206	0.3	7.8(30)
Segment (reinforced concrete)	34.5	0.18	2.8

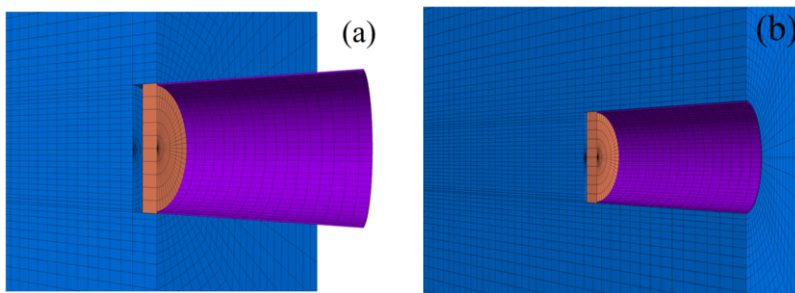
### 3.2. Refined Modeling Process



**Figure 1.** Axisymmetric numerical calculation model

The calculation employs an axisymmetric model as depicted in Figure 1. The model has dimensions of 60m, 30m, and 60m along the tunnel axis for length, width, and height, respectively. The rock mass is modeled using an ideal elastic-plastic constitutive model with a Mohr-Coulomb yield criterion. Constraints are applied to the bottom of the model in the Z direction, to the two outer surfaces along the X axis for displacement, and to the two outer surfaces along the cavity axis (Y axis) in the Y direction. Initial stress is added to the elements based on the inversion analysis results of the initial ground stress under the environment of the cavity segment. Corresponding normal stress is applied to the upper surface of the model in the Z axis.

During actual engineering, the tunneling process of shield tunneling machines is considered to be continuous excavation. However, simulating the tunneling process using FLAC3D simulation software can be challenging to achieve the continuous advancement of the shield construction. Therefore, the excavation process of the shield tunneling machine is considered as a discontinuous process in this study. After extensive research, an automatic simulation technology for the tunneling process of shield tunneling machines has been developed. The specific steps for this technology are illustrated in Figure 2:



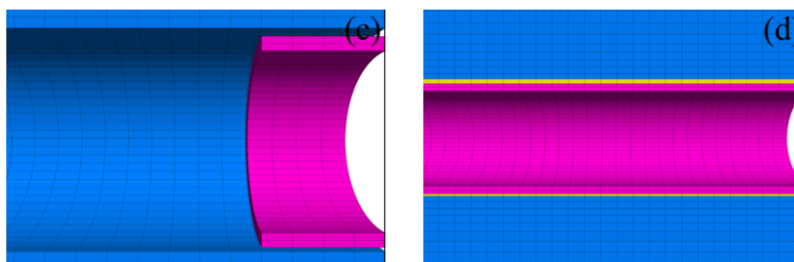


**Figure 2.** Refined Simulation of Shield Tunneling Process

(1) The inversion data of the geostress field in the tunnel area are directly read into the calculation model and calculated to the stress balance.

(2) Start the cutter head, and the shield enters the hole. In accordance with the mesh division accuracy, dig 1.5m each time along the axis of the hole, and apply stress perpendicular to the work face to simulate the cutter head thrust. The stress is the sum of the soil pressure and water pressure of the work face facing the cutter head in the driving process, and it is realized by applying the same amount of force in the opposite direction to the grid points on the work face. This force is applied on the next face after each cycle, and the cutter head thrust applied in the previous cycle is removed accordingly.

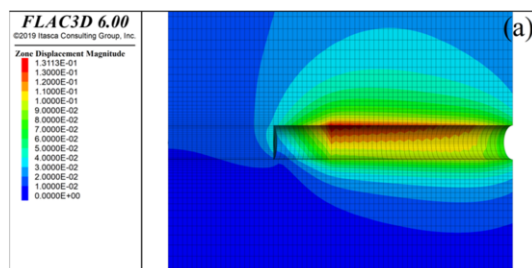
(3) Lining installation and grouting backfill. When the shield machine completely enters the rock mass, the segment lining is installed at the rear of the backing and the backfill process begins.

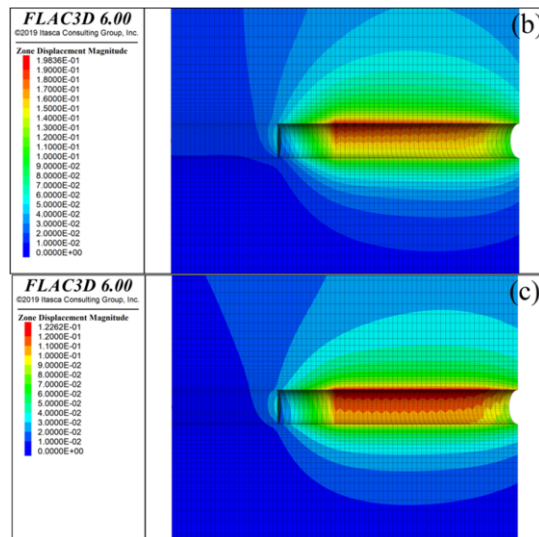
(4) Conduct a cyclic tunneling process simulation of the shield tunneling machine and simultaneously monitor the interaction force of the surrounding rock on the outer surface of the shield.

#### 4. Calculation Results and Analysis

Figure 3 to Figure 5 display the calculated deformation and stress characteristics of the surrounding rock and supporting structure. In each figure, (a), (b), and (c) represent the results of typical cave sections in Shenhe tableland, Shaoling tableland, and Bailu tableland, respectively.

##### 4.1. Deformation Characteristics of Surrounding Rock

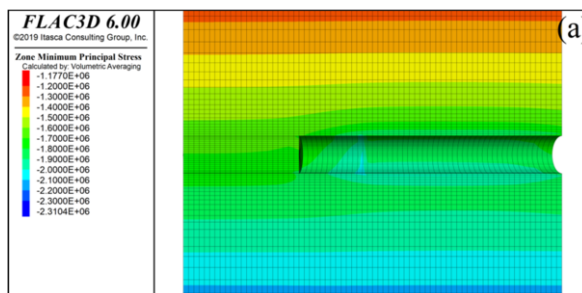


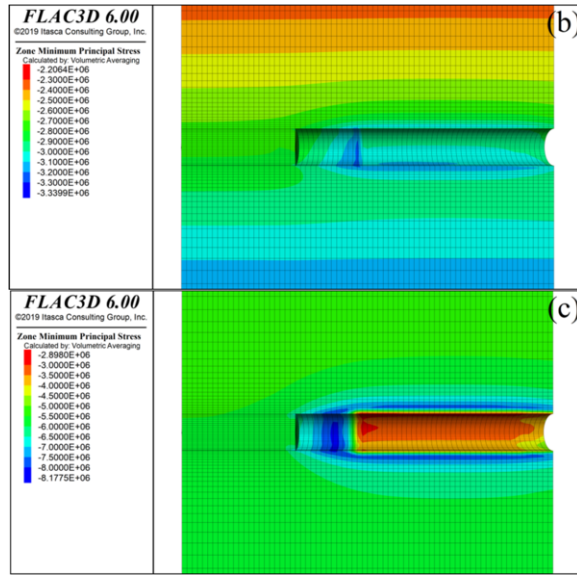


**Figure 3.** Surrounding rock deformation nephogram of typical tunnel section

Observing Figure 3, it can be inferred that the surrounding rock of complex loess possesses poor self-stability, which leads to difficult cave formation after excavation and significant displacement of surrounding rock as a whole. At the work face, the rock and soil mass undergoes noticeable deformation due to the action of the cutter head driving thrust. Despite the displacement being relatively low at the cutter head, the surrounding rock deformation from the back of the hand surface to the tube segment gradually increases, owing to the supporting effect of the work face. The junction of the shield tail and the segment structure exhibits the maximum value of the surrounding rock deformation, with values of 13.11cm and 19.84cm in Shenhe Tablelands and Shaoling Tablelands, respectively. In the cave section of Bailu Tableland, the maximum value of surrounding rock deformation is 12.26cm. It is worth noting that the types of surrounding rock in some cave sections of Bailu Tableland are better, leading to relatively smaller deformation of surrounding rock under the condition of a larger overall buried depth. For a single section of the surrounding rock of the tube fragment, the deformation gradually reduces from the tunnel wall to the lateral rock mass, and the upper rock mass exhibits comparatively more deformation.

#### 4.2. Mechanical Characteristics of Surrounding Rock

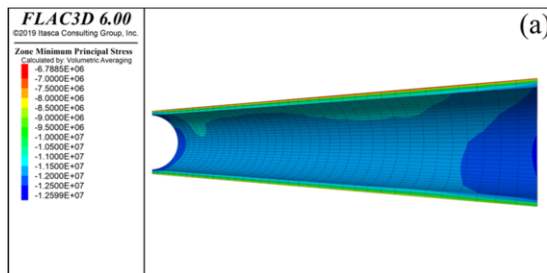




**Figure 4.** Nephogram of maximum principal stress of surrounding rock in typical tunnel section

Based on Figure 4, it can be observed that the shield excavation causes stress redistribution in the surrounding rock within a certain range of the reserved gap at the shield. In terms of secondary stress, the highest maximum principal stress value is found near the shield tail. The maximum principal stress of the surrounding rock in Shenhe Tableland is 2.31 MPa, in Shaoling Tableland is 3.34 MPa, and in the cave section of Bailu Tableland is 8.18 MPa. The segment structure provides support to the surrounding rock, and the maximum principal stress on the upper surface of the surrounding rock in contact with the segment is lower than that on the lower surface in Shenhe Tableland and Shaoling Tableland. The stress distribution around the cave in Bailu Tableland is relatively uniform, but there is a stratiform stress distribution phenomenon observed from the cave wall to the lateral rock mass, such as stress release zone, concentration zone, transition zone, and no interference zone.

#### 4.3. The Force Characteristics of the Supporting Structure



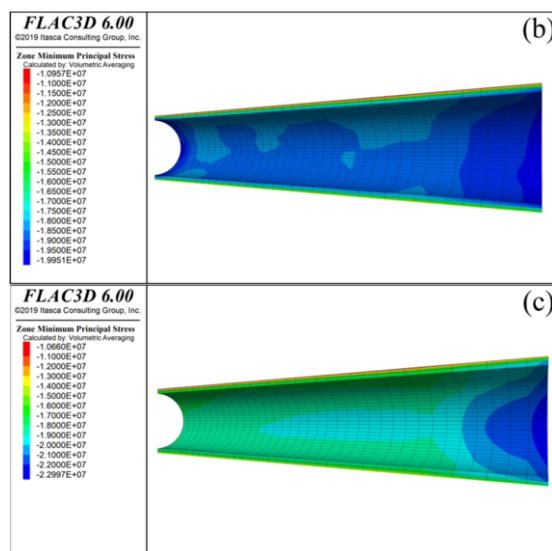


**Figure 5.** Maximum principal stress nephogram of typical tunnel support structure

From Figure 5, it can be observed that the maximum principal stress is relatively high at the junction of the shield tail and segment structure, as well as at the entrance, in the tunneling direction of the tunnel. Furthermore, the maximum principal stress of each typical tunnel segment increases with the increase in buried depth. The maximum principal stress of the support structure in Shenhe Tableland tunnel segment is 12.60 MPa, in Shaoling Tableland is 19.95 MPa, and in the cave section of Bailu Tableland is 22.30 MPa. However, these values are lower than the design value of the segment materials used in engineering design, indicating that the risk of shear failure of the segment structure is low under this working condition. The stress in the middle segment of each tunnel is relatively uniform, and the maximum principal stress of the roof is relatively small at the single section of the segment.

## 5. Conclusion

The process of shield tunneling and backfilling support was simulated using the numerical analysis software FLAC3D. Based on the geological survey data, the mechanical characteristics of complex geological segment structures were analyzed for selected cave segments in the maximum buried depth of Shenhe Tableland, Shaoling Tableland, and Bailu Tableland of the South Main Line. The following conclusions were drawn from the analysis:

(1). The surrounding rock of complex loess has poor self-stability, and it is difficult to form caves after excavation, resulting in large displacement of surrounding rock as a whole. The rock and soil mass at the work face appears obvious deformation under the action of cutter head driving thrust. On the whole, due to the supporting effect of the work face, the displacement at the cutter head is small, and the surrounding rock deformation from the back of the work face to the tube segment gradually increases.

(2). The unloading effect of shield excavation leads to stress redistribution in the surrounding rock within a certain range of the shield gap, resulting in a higher maximum

principal stress in the secondary stress near the shield tail. In the Bailu Tableland section, cyclic stress distribution phenomena such as stress release zone, concentration zone, transition zone, and non-interference zone can be observed from the wall to the outer rock mass.

(3). In the direction of tunneling, the maximum principal stress is highest at the junction of the shield tail and segment structure, as well as at the tunnel entrance. Conversely, the stress in the middle of the tunnel segment is relatively uniform. Additionally, the maximum principal stress on the roof of the tunnel segment is relatively low.

## Acknowledgments

This work was financially supported by grants from the Natural Science Foundation of Shaanxi Province (Grant Nos. 2021JLM-50 and 2019JLZ-13).

## References

- [1] Bobet A 2001 Analytical solutions for shallow tunnels in saturated ground *J. Journal of Engineering Mechanics* **127** 1258-66
- [2] Lv X L, Zhou Y C, Huang M S and Zeng S 2018 Experimental study of the face stability of shield tunnel in sands under seepage condition *J. Tunnelling and Underground Space Technology* **74** 195-205
- [3] Park K H 2004 Elastic solution for tunneling-induced ground movements in clays *J. International Journal of Geomechanics* **4** 310-18
- [4] Finno R J and Clough G W 1985 Evaluation of soil response to EPB shield tunneling *J. Journal of Geotechnical Engineering* **111** 157-173
- [5] Li Y, Emeriault F, Kastner R and Zhang Z X 2009 Stability analysis of large slurry shield-driven tunnel in soft clay *J. Tunnelling and Underground Space Technology* **24** 472-81
- [6] Huang D W, Jiang H, Xu C J, Yu W B, Li X and Wang W 2022 A new design method of shield tunnel based on the concept of minimum bending moment *J. Applied Sciences* **12** 1082
- [7] Yi H W and Sun J 2000 Mechanism analysis of disturbance caused by shield tunneling on soft clays *J. Journal of Tongji University* **28** 277-81
- [8] Rowe R K and Lee K M 1992 An evaluation of simplified techniques for estimating three-dimensional untrained ground movements due to tunneling in soft soils *J. Canadian Geotechnical Journal* **29** 39-52
- [9] Chen R P, Tang L J, Ling D S and Chen Y M 2011 Face stability analysis of shallow shield tunnels in dry sandy ground using the discrete element method *J. Computers and Geotechnics* **38** 187-195
- [10] Kirsch A 2010 Experimental investigation of the face stability of shallow tunnels in sand *J. Acta Geotechnica* **5** 43-62
- [11] Feng K, He C and Xia S L 2011 Prototype tests on effective bending rigidity ratios of segmental lining structure for shield tunnel with large cross-section *J. Chinese Journal of Geotechnical Engineering* **33** 1750-1758
- [12] Fang Y, Chen Z T, Tao L M, Cui J and Yan Q X 2019 Model tests on longitudinal surface settlement caused by shield tunnelling in sandy soil *J. Sustainable Cities and Society* **49** 101504